

*Biogeosciences Discussions* is the access reviewed discussion forum of *Biogeosciences*

**Dissolved Organic  
Nitrogen and primary  
production**

G. Charria et al.

# Importance of dissolved organic nitrogen in the North Atlantic Ocean in sustaining primary production: a 3-D modelling approach

G. Charria<sup>1,2</sup>, I. Dadou<sup>1</sup>, J. Llido<sup>1,3</sup>, M. Drévillon<sup>1,4</sup>, and V. Garçon<sup>1</sup>

<sup>1</sup>Laboratoire d'Etudes en Géophysique et Océanographie Spatiales, UMR5566/CNRS, Toulouse, France

<sup>2</sup>National Oceanography Centre, Southampton, UK

<sup>3</sup>Institute for Marine and Atmospheric research Utrecht (IMAU), Utrecht, The Netherlands

<sup>4</sup>CERFACS, Toulouse, France

Received: 17 March 2008 – Accepted: 20 March 2008 – Published: 17 April 2008

Correspondence to: G. Charria (gcha@noc.soton.ac.uk)

Published by Copernicus Publications on behalf of the European Geosciences Union.

Title Page

Abstract

Introduction

Conclusions

References

Tables

Figures

◀

▶

◀

▶

Back

Close

Full Screen / Esc

Printer-friendly Version

Interactive Discussion



## Abstract

An eddy-permitting coupled ecosystem-circulation model including dissolved organic matter is used to estimate the dissolved organic nitrogen (DON) supply sustaining primary production in the subtropical North Atlantic Ocean.

After an analysis of the coupled model performances compared to the data, a sensitivity study demonstrates the strong impact of parameter values linked to the hydrolysis of particulate organic nitrogen and remineralisation of dissolved organic nitrogen on surface biogeochemical concentrations.

The physical transport of dissolved organic nitrogen contributes to maintain the level of primary production in this subtropical gyre. It is dominated by the meridional component. We estimate a meridional net input of  $0.039 \text{ molN.m}^{-2}.\text{yr}^{-1}$  over the domain ( $13^{\circ}$ – $35^{\circ}$  N and  $71$ – $40^{\circ}$  W) in the subtropical gyre. This supply is driven by the Ekman transport in the southern part and by non-Ekman transport (meridional current components, eddies, meanders and fronts) in the northern part of the subtropical gyre. At  $12^{\circ}$  N, our estimate ( $18 \text{ kmolN.s}^{-1}$ ) confirms the estimation ( $17.9 \text{ kmolN.s}^{-1}$ ) made by Roussenov et al. (2006) using a simplified biogeochemical model in a large scale model. This DON meridional input is within the range (from  $0.05$  up to  $0.24 \text{ molN.m}^{-2}.\text{yr}^{-1}$ ) (McGillicuddy and Robinson, 1997; Oschlies, 2002) of all other possible mechanisms (mesoscale activity, nitrogen fixation, atmospheric deposition) fuelling primary production in the subtropical gyre. The present study confirms that the lateral supply of dissolved organic nitrogen might be important in closing the N budget over the North Atlantic Ocean and quantifies the importance of meridional input of dissolved organic nitrogen.

## 1 Introduction

The subtropical gyres cover large regions of the ocean (40% of the global ocean, McClain et al., 2004). They represent a significant contribution of the biological pump of carbon in the global ocean estimated around 50% (Emerson et al., 1997). The

**BGD**

5, 1727–1764, 2008

## Dissolved Organic Nitrogen and primary production

G. Charria et al.

Title Page

Abstract

Introduction

Conclusions

References

Tables

Figures

◀

▶

◀

▶

Back

Close

Full Screen / Esc

Printer-friendly Version

Interactive Discussion



## Dissolved Organic Nitrogen and primary production

G. Charria et al.

Title Page

Abstract

Introduction

Conclusions

References

Tables

Figures

◀

▶

◀

▶

Back

Close

Full Screen / Esc

Printer-friendly Version

Interactive Discussion



North Atlantic subtropical gyre is an example of these oligotrophic areas where inorganic nutrients concentrations are depleted and where the primary production (about  $100 \text{ gC.m}^{-2}.\text{yr}^{-1}$  or  $1.26 \text{ molN.m}^{-2}.\text{yr}^{-1}$ , Ducklow, 2003) in the first 100 m depth is moderate. However, even if this production is weak, the extension of the subtropical gyre is quite important for the entire North Atlantic Ocean and has expanded over the 1996–2003 period (+4% per year – McClain et al., 2004). Several unknowns remain on the sources of nutrients to sustain the primary production in the subtropical gyres. For the North Atlantic Ocean, the following four main mechanisms could be at work: (1) Transport of nutrients by mesoscale activity (i.e. eddies, meanders, fronts) ranging from 0.05 to  $0.24 \text{ molN.m}^{-2}.\text{yr}^{-1}$  (i.e. McGillicuddy and Robinson, 1997; Siegel et al., 1999; Oschlies, 2002), (2) Meridional Ekman transport of dissolved organic matter slowly remineralized from the enriched boundaries of the oligotrophic gyre (i.e. Williams and Follows, 1998; Roussenov et al., 2006), for example around  $0.047 \text{ molN.m}^{-2}.\text{yr}^{-1}$  in the subtropical gyre (Mahaffey et al., 2004), (3) Transport of nutrients and dissolved organic matter from the coastal upwelling areas (i.e. Mauritanian upwelling – Roussenov et al., 2006) (4) Biological fixation of  $\text{N}_2$  gas ranging from 0.025 to  $0.07 \text{ molN.m}^{-2}.\text{yr}^{-1}$  (i.e. Gruber and Sarmiento, 1997; Hansell et al., 2004). All these processes represent possible candidates for sustaining primary production in the North Atlantic Ocean subtropical gyre.

In the present study, we investigate the importance of dissolved organic matter for fuelling primary production. In particular, the different meridional transports (Ekman and non-Ekman) are examined using a coupled physical/biogeochemical model covering the North Atlantic Ocean. The following questions are addressed: How are the surface concentrations sensitive to the choice of the model parameter values, especially those associated with dissolved organic matter? What are the sources of the available dissolved organic nitrogen to sustain primary production?

After a description of the coupled model and of the in situ and remotely sensed data used, a model/data comparison is presented, which emphasizes the strong and weak points of the modelled fields. Sensitivity experiments are then performed showing the

central role of processes linked to the dissolved organic matter. In the last section, the mechanisms associated with this organic matter are assessed and compared with previous studies in the North Atlantic Ocean.

## 2 Methodology

### 2.1 Coupled physical/biogeochemical model

The physics and dynamics of the ocean circulation are simulated using the OPA numerical model (8.1 version, Madec et al., 1999) in a North Atlantic Ocean configuration referred to as MNATL. This model was initially developed within the CLIPPER project by Barnier et al. (2000) and Tréguier et al. (2001) and used by the operational oceanography project MERCATOR (<http://www.mercator-ocean.fr>). The primitive equations are solved using hydrostatic and rigid lid approximations. The TKE turbulent closure scheme (Blanke and Delecluse, 1993) is applied to calculate the vertical mixing of momentum and tracers. The MNATL configuration is restricted to the North Atlantic Ocean from 20° S to 70° N and from 98.5° W to 20° E. A restoring term to the Reynaud et al. (1998) climatology for temperature and salinity was introduced in the Gulf of Cadix (Drillet et al., 2005). The horizontal grid is a Mercator projection: the horizontal resolution of 1/3° is modulated by the cosine of the latitude (i.e. 30 km at 35° N). The model has 43 z-levels on the vertical among which 20 lie in the first 1000 m of the ocean. The levels are about 12 m apart in the upper ocean and 200 m apart below 1500 m. The model is forced with the ECMWF daily ocean-atmosphere fluxes. The Sea Surface Temperature (SST) and Sea Surface Salinity (SSS) are restored to the weekly Reynolds's analysis (Reynolds and Smith, 1994) and to seasonal Reynaud et al.'s (1998) climatology, respectively.

To keep the model as simple as possible and in the mean time capture essential biogeochemical features in the North Atlantic Ocean (i.e., the spring bloom, the regenerated production in the oligotrophic gyre as well as exported production), the biogeo-

**BGD**

5, 1727–1764, 2008

## Dissolved Organic Nitrogen and primary production

G. Charria et al.

Title Page

Abstract

Introduction

Conclusions

References

Tables

Figures

◀

▶

◀

▶

Back

Close

Full Screen / Esc

Printer-friendly Version

Interactive Discussion



## Dissolved Organic Nitrogen and primary production

G. Charria et al.

Title Page

Abstract

Introduction

Conclusions

References

Tables

Figures

◀

▶

◀

▶

Back

Close

Full Screen / Esc

Printer-friendly Version

Interactive Discussion



chemical model of Huret et al. (2005) was used. It includes 5 state variables: Phytoplankton (P), Zooplankton (Z), Dissolved Inorganic Nitrogen (N), Particulate Organic Nitrogen or Detritus (D) and Dissolved Organic Nitrogen (DON) (Fig. 1). The modelled DON is the semi-labile DON. The refractory pool of DON and the labile DON are not considered in these simulations, because their turnover rates are too long (hundred of years) and too short (less than a day), respectively. This model is coupled with the MNATL circulation model previously described (see Huret et al., 2005, for a detailed description of the model). The MUSCL (Monotonic Upstream centred Scheme for Conservation Laws) advection scheme was used for the biogeochemical tracers (Estubier and Levy, 2000). With this scheme, the errors of diffusion and dispersion, which result in unrealistic negative concentrations, are minimized.

The parameter values (Table 1) are deduced from Oschlies and Garçon (1999) and Huret (2005). A preliminary sensitivity study and data comparison were performed and led to new values for remineralisation and hydrolysis rates (Charria, 2005). In this nitrogen based model, all tracers concentrations are expressed in nitrogen currency ( $\text{mmolN}\cdot\text{m}^{-3}$ ). A variable chlorophyll-to-nitrogen ratio was used following Hurtt and Armstrong (1996) to convert modelled phytoplankton in nitrogen units into chlorophyll concentrations using the formulation:

$$\text{Chl} = 1.59 \cdot \chi \cdot P \quad (1)$$

with  $P$  for phytoplankton concentration in  $\text{mmolN}\cdot\text{m}^{-3}$ , Chl for chlorophyll concentration in  $\text{mgChl}\cdot\text{m}^{-3}$  and 1.59 for the standard chlorophyll to nitrogen ratio. If growth is light limited, then  $\text{Chl}/\text{N} = 1.59 \cdot \chi_{\text{max}}$  which means Chl/N is maximum. We chose  $\chi_{\text{max}}$  equal to 1 which gives a  $\text{C}/\text{Chl}_{\text{min}}$  of  $25 \text{ gC} \cdot (\text{gChl})^{-1}$ . If phytoplankton is nutrient limited, we adjust  $\chi$  downwards to make it equally limited by light and nutrients. We neglect the effect of  $\chi$  on the light profile and then the growth rate limited by light is a linear function of  $\chi$ . Therefore,  $\chi$  is simply given by  $\chi = \text{nutrient limited growth rate} / \text{light limited growth rate}$ . We choose to fix the upper limit for the  $(\text{C}/\text{Chl})_{\text{max}}$  equal to 160.

The interannual simulation is initialized in temperature and salinity from the Reynaud

et al.'s (1998) climatology for the circulation model. Initial conditions for dissolved inorganic nitrogen are taken from the nitrate climatology of Conkright et al. (1998). The other biogeochemical state variables are initialized to fixed values in space (longitude and latitude) as in Sarmiento et al. (1993) and Oschlies and Garçon (1999). The initial conditions for P, Z, DON are  $0.14 \text{ mmolN.m}^{-3}$ ,  $0.014 \text{ mmolN.m}^{-3}$  and  $3 \text{ mmolN.m}^{-3}$  at the surface, respectively, decreasing exponentially with a scale depth of 100 m. D is initialized with a small value everywhere ( $10^{-4} \text{ mmolN.m}^{-3}$ ). The physical model alone has been integrated since 1 January 1995. After one year of integration, the coupled model has been integrated for two years (1996–1997). After this two years spin-up, the third year (from 1 January 1998) is analyzed. The biogeochemical fields are then spun-up with an established seasonal cycle.

### 3 Data used

Different data types have been used to compare with the model fields: satellite data, cruise sections through the North Atlantic basin as well as in situ data at moored stations. We focus on 1998 when all types of data previously listed are available except for WOCE (World Ocean Circulation Experiment) sections and EUMELI station (Fig. 2). We use the WOCE sections for the year 1997 as the physical structures are well simulated and the nitrate concentrations do not seem to change significantly between mid-1997 and 1998. Satellite chlorophyll-*a* concentrations from monthly SeaWiFS products of level 3 binned data ( $9 \times 9 \text{ km}$ , version 4, O'Reilly et al., 2000) and in situ chlorophyll data (Ducklow, 2003) are compared to modelled chlorophyll concentrations on the first vertical level (6 m) of the model. Integrated modelled primary production over the euphotic zone is also assessed using primary production estimations from SeaWiFS data and three bio-optical models (Carr et al., 2006). Along WOCE (end of 1997) and AMT (Atlantic Meridional Transect) sections (in 1998) (Aiken and Bale, 2000), temperature (*T*), salinity (*S*), nitrates ( $\text{NO}_3$ ) and chlorophyll (Chl) concentrations are compared with model outputs for the same locations and periods. At BATS

**BGD**

5, 1727–1764, 2008

## Dissolved Organic Nitrogen and primary production

G. Charria et al.

Title Page

Abstract

Introduction

Conclusions

References

Tables

Figures

◀

▶

◀

▶

Back

Close

Full Screen / Esc

Printer-friendly Version

Interactive Discussion



(Bermuda Atlantic Time-series Study) station (31°40'N, 64°10'W) on the western part of the basin (e.g. Steinberg et al., 2001), an exhaustive comparison is performed between the available data and model fields for  $T$ ,  $S$ ,  $\text{NO}_3$ , Chl, and dissolved organic nitrogen (DON). On the eastern part of the basin, the oligotrophic EUMELI (France-JGOFS EUtrophic, MEsotrophic and oLigotrophic program) station data for the years 1991 and 1992 (Morel et al., 1996) have been put together to create a combined year with which the model fields are compared.

Statistical metrics are selected in order to compare model fields and data: the mean ( $M$ ), the bias ( $M_{\text{model}} - M_{\text{data}}$ ), the root mean square (RMS), the centred pattern RMS difference ( $E' = \sqrt{\text{RMS}^2 - \text{bias}^2}$ ), the standard deviation ( $\sigma$ ) and the correlation ( $R$ ). Taylor's diagrams (Taylor, 2001) are used in order to summarize the statistical information ( $\sigma$ ,  $R$ ,  $E'$ ).

## 4 Model-data comparisons

### 4.1 Salinity, temperature and density

Along the WOCE sections, the difference between model and data averages (along the section and over the first 500 m depth) are from  $-0.26^\circ\text{C}$  to  $-0.65^\circ\text{C}$  and from  $-0.008$  psu to  $-0.12$  psu. For the AMT sections over the oligotrophic gyre, the difference between model and data averages (along the section and over the first 200-meters depth) are from  $-0.13^\circ\text{C}$  to  $-1.015^\circ\text{C}$ ; from  $-0.18$  psu to  $-0.185$  psu. At BATS station, the differences between model and data averages (for the year 1998 and over the first 300-meters depth) are equal to  $-0.61^\circ\text{C}$  and  $-0.15$  psu. In general, the modelled mean temperature and salinity is thus usually colder and fresher, respectively, than the observation mean. The standard deviation is also usually higher for the observed fields compared to the simulated fields (Fig. 3). The model spatial resolution of  $1/3^\circ$  is too coarse to reproduce the highly variable small-scale processes. The correlation coefficient for temperature ( $T$ ) between simulated and observed fields is above 90% for

**BGD**

5, 1727–1764, 2008

## Dissolved Organic Nitrogen and primary production

G. Charria et al.

Title Page

Abstract

Introduction

Conclusions

References

Tables

Figures

◀

▶

◀

▶

Back

Close

Full Screen / Esc

Printer-friendly Version

Interactive Discussion



BATS station and all sections except for the A02 WOCE section (Fig. 3a). The normalized centred pattern RMS difference for  $T$  is less than 0.5 (less than  $2.2^{\circ}\text{C}$ ) except for two WOCE sections (A20 and A02). For the salinity ( $S$ ) field, a clear distinction can be seen between the sections/station on the western part of the basin or near  $40^{\circ}\text{N}$  compared to the sections on the eastern part of the basin or at other latitudes. For the latter, the correlation coefficient between simulated and observed fields is above 90%; the standard deviation of the modelled and observed fields is similar and the normalized centred pattern RMS difference is less than 0.5 (less than 0.23 psu). On the western part of the basin, the statistics show a weaker agreement with observations and particularly, with the extreme case of the BATS station (Fig. 3b). The simulated density field is comparable to the observed one along the sections and at BATS station due to the compensation in density of the discrepancies in  $T$  and  $S$  (Fig. 3c).

As an example, simulated and observed distributions of  $T$  and  $S$  over the 350 m depth along the A22 WOCE section (North-South direction around  $66^{\circ}\text{W}$  in August 1997 – Fig. 2) are displayed in Fig. 4. This meridian section crosses the subtropical gyre on its western part which is well identified by warm (up to  $28^{\circ}\text{C}$ ) and salty (up to 37 psu) waters between  $13.2^{\circ}\text{N}$  and  $39^{\circ}\text{N}$  in the observed and simulated fields (Fig. 4) above the first 200 m. Below 200 m, the North Atlantic Central Waters (NACW) (with  $T$  near  $20^{\circ}\text{C}$  and  $S$  near 36.7 psu) between  $39^{\circ}\text{N}$  and  $13.2^{\circ}\text{N}$  can be identified. In the observed fields, colder and fresher water is found north of  $39^{\circ}\text{N}$ , characterizing the Slope Water, north of the Gulf Stream current. In the simulated fields, these waters are found north of  $41^{\circ}\text{N}$ . In our  $1/3^{\circ}$  of resolution with z-vertical coordinate configuration, the northern position of the Gulf Stream current is a well-known bias (e.g. Barnier et al., 2006). The temperature and salinity gradients in the simulated fields are weaker than in the observed fields. The simulated sea surface temperature in the subtropical gyre is colder than the observed SST. A detailed analysis of the North Atlantic Subtropical Mode Water (STMW – characterized by a subsurface thermostat centred roughly at  $18^{\circ}\text{C}$ ) between 150 and 400 m at different stations along this A22 section shows that the STMW is not well reproduced in the simulated fields (not shown). This bias is linked

## Dissolved Organic Nitrogen and primary production

G. Charria et al.

Title Page

Abstract

Introduction

Conclusions

References

Tables

Figures

◀

▶

◀

▶

Back

Close

Full Screen / Esc

Printer-friendly Version

Interactive Discussion



to the northern position of the Gulf Stream current because this mode water is formed south of this current (Palter et al., 2005).

Along the AMT 6 section (from 24 May 1998 to 14 June 1998) between 0° N and 50° N in the eastern part of the North Atlantic basin (see Fig. 2), the subtropical gyre waters are well represented in the coupled model compared to the observations. We only notice an underestimation of the Mauritanian upwelling and salinity values (no subsurface subtropical salinity maximum at 37 psu) (Fig. 5.1). At the equator, we can notice fresher waters associated with the Amazon River discharge waters. Indeed, these waters are advected eastward by the North Equatorial Counter Current and mixed with the equatorial upwelling waters (Aiken and Bale, 2000). They are well reproduced in the simulated salinity fields.

The model is able to reproduce the large-scale features of the temperature, salinity and density fields, however the modelled fields are generally fresher and colder than the observations partly due to the northern position of the Gulf Stream current.

## 4.2 Nitrate and chlorophyll concentrations

In this section, the nitrate and chlorophyll concentrations are averaged over the corresponding vertical section (WOCE and AMT) or over the corresponding time series (BATS and EUMELI).

The modelled mean nitrate and chlorophyll concentrations are higher than the observation mean over the WOCE sections ( $0.57 \text{ mmolN.m}^{-3} \leq [\text{NO}_3]_{\text{model}} - [\text{NO}_3]_{\text{data}} \leq 0.7 \text{ mmolN.m}^{-3}$ ), the AMT sections ( $[\text{NO}_3]_{\text{model}} - [\text{NO}_3]_{\text{data}} = 1.5 \text{ mmolN.m}^{-3}$ ;  $0.034 \text{ mgChl.m}^{-3} \leq [\text{Chl}]_{\text{model}} - [\text{Chl}]_{\text{data}} \leq 0.096 \text{ mgChl.m}^{-3}$ ) and at BATS station ( $[\text{NO}_3]_{\text{model}} - [\text{NO}_3]_{\text{data}} = 4.4 \text{ mmolN.m}^{-3}$ ;  $[\text{Chl}]_{\text{model}} - [\text{Chl}]_{\text{data}} = 0.13 \text{ mgChl.m}^{-3}$ ). The highest mean bias is obtained at BATS in agreement with the bad representation of the thermohaline waters properties in this area as mentioned above. We also compare the model outputs with the observations at the EUMELI site. Even if the period of the EUMELI survey (1991–1992) is not the same than the simulated year

## Dissolved Organic Nitrogen and primary production

G. Charria et al.

Title Page

Abstract

Introduction

Conclusions

References

Tables

Figures

◀

▶

◀

▶

Back

Close

Full Screen / Esc

Printer-friendly Version

Interactive Discussion



(1998) (see part 2.2), this site is considered due to its location within the oligotrophic waters. For this site (21° N, 31° W), the simulated nutrient mean concentration over the year 1998 is higher than the observed nitrate mean over the years 1991–1992 ( $[\text{NO}_3]_{\text{model}} - [\text{NO}_3]_{\text{data}} = 1.22 \text{ mmolN.m}^{-3}$ ) and simulated chlorophyll concentrations are slightly underestimated ( $[\text{Chl}]_{\text{model}} - [\text{Chl}]_{\text{data}} = -0.08 \text{ mgChl.m}^{-3}$ ).

The standard deviation is also higher at EUMELI for the observed fields as compared to the simulated fields even if this difference is not as clear as for the *T* and *S* fields (Fig. 6).

The correlation coefficient for nutrients between simulated and observed fields range between 35% and 90%; a higher correlation is obtained for the eastern part of the North Atlantic Ocean (Fig. 6a). The correlation for the chlorophyll concentrations is weaker (less than 40%) (Fig. 6b). It is mainly due to a different vertical chlorophyll distribution as simulated by the model with shallower subsurface maximum and higher amplitude of the annual chlorophyll cycle in the oligotrophic gyre (not shown here).

The normalized centred pattern RMS difference for nutrients and chlorophyll concentrations are between 0.4 and 1.2 (between 1 and 5.5  $\text{mmolN.m}^{-3}$ ) and between 1 and 1.6 (between 0.16 and 0.57  $\text{mgChl.m}^{-3}$ ) (Fig. 6).

Along the A22 WOCE section, the observed nitrate concentrations are very low in the waters of the subtropical oligotrophic gyre between 13.17° N and 39° N. These concentrations are rather well simulated by the model except the vertical gradients, which are smoother than in the observations (Fig. 4).

For the AMT6 section, the simulated nitrate field structures compare well with the observed structures except the northern border of the oligotrophic gyre, which has a too southern position as compared to the data (Fig. 5.2). For example, at 36.6° N, the observed nitrate concentrations are less than 5  $\text{mmolN.m}^{-3}$  whereas the simulated dissolved inorganic nitrogen concentrations are around 10  $\text{mmolN.m}^{-3}$ . The enriched nitrate waters of the Mauritania upwelling (between 12.8° N and 20.4° N) and of the Equatorial upwelling are well reproduced in the simulated fields. The chlorophyll concentrations at the southern and northern borders of the oligotrophic gyre are too high

**Dissolved Organic Nitrogen and primary production**

G. Charria et al.

Title Page

Abstract

Introduction

Conclusions

References

Tables

Figures

◀

▶

◀

▶

Back

Close

Full Screen / Esc

Printer-friendly Version

Interactive Discussion



as compared to the observations (Fig. 5.2).

The model slightly overestimates chlorophyll and dissolved inorganic nitrogen concentrations. However the seasonal annual cycle and the main patterns of the vertical structure are well reproduced.

#### 5 4.3 Surface chlorophyll concentrations and primary production

After using in situ data (along sections and at fixed stations), the synoptic 9-km-resolution monthly SeaWiFS data have been used to compare chlorophyll concentrations in surface waters. Over the North Atlantic basin for the year 1998, the simulated chlorophyll concentrations are underestimated as compared to the data (mean over the basin:  $[\text{Chl}]_{\text{model}} - [\text{Chl}]_{\text{data}} = -0.134 \text{ mgChl.m}^{-3}$ ), especially at high latitudes (Fig. 7). The correlation is very low (13%) and the normalized centred pattern RMS difference is high ( $0.98 \text{ mgChl.m}^{-3}$ ) for the whole basin (Fig. 6b). These poor statistics can be explained examining the chlorophyll concentration distribution over the North Atlantic Ocean, for example for the spring bloom season (Fig. 7). First, the weakest latitudinal extension of the oligotrophic gyre strongly decreases the correlation between modelled and remotely sensed chlorophyll concentrations. Indeed, the northern border of the oligotrophic gyre as simulated by the model has a southernmost position as compared to the data. The reduced oligotrophic gyre extension in its northern boundary could be partly associated with the misrepresentation of the STMW, characterized by low dissolved inorganic nitrogen concentrations (Palter et al., 2005).

Secondly, in the northern part of the basin, the bloom has a patchy structure, which is difficult to reproduce. This patchiness of the bloom is partly due to small-scale physical processes, which are not solved in our model with a  $1/3^\circ$  spatial resolution. Nevertheless, simulations present a good agreement with observations in magnitude. The spring bloom period is quite well represented in the simulated chlorophyll concentrations fields as well as the seasonal variability (not shown).

Following the study by Ducklow (2003), in Table 2, we compare the integrated (over 112 m depth during the year 1998) simulated primary production (PP) with different

## Dissolved Organic Nitrogen and primary production

G. Charria et al.

Title Page

Abstract

Introduction

Conclusions

References

Tables

Figures

◀

▶

◀

▶

Back

Close

Full Screen / Esc

Printer-friendly Version

Interactive Discussion



---

**Dissolved Organic Nitrogen and primary production**

---

G. Charria et al.

---

Title Page

Abstract

Introduction

Conclusions

References

Tables

Figures

◀

▶

◀

▶

Back

Close

Full Screen / Esc

Printer-friendly Version

Interactive Discussion



estimations of PP from in situ data (during the JGOFS cruises from 1986 to 1999 and integrated to the base of the euphotic zone; Ducklow, 2003) and satellite data (based on 1978 to 1986 data in Antoine and Morel, 1996; based on 1971 to 1994 measurements in Behrenfeld and Falkowski, 1997; based on 1998 to 2002 measurements in Mélin, 2003) over the different biogeochemical provinces defined by Longhurst (1998). For the polar region (Atlantic Arctic Province – ARCT and Atlantic Subarctic Province – SARC) as well as in the North Atlantic Drift Province (NADR), the modelled PP (around  $230 \text{ mgC.m}^{-2}.\text{d}^{-1}$ ) is underestimated. PP is mainly limited by light at these latitudes. The simulated convection is higher in these provinces than the convection that can be estimated from the observations (e.g. Barnier et al., 2006), which partly explain this underestimation. Another explanation is that the model does not explicitly resolve the diurnal cycle, and the day light forcing could be improved using a higher frequency forcing (i.e. 6 h). In the Gulf Stream province, the PP, equal to  $363 \text{ mgC.m}^{-2}.\text{d}^{-1}$ , is also underestimated as compared with the satellite estimation (Table 2). This difference can be due to the coarse  $1/3^\circ$  horizontal resolution of the model that does not allow to properly reproduce the most intense mesoscale processes commonly observed in this energetic region. In the North Atlantic Subtropical Gyral provinces (East – NASE and West – NASW), the modelled PP ( $392 \text{ mgC.m}^{-2}.\text{d}^{-1}$  in the NASE and  $448 \text{ mgC.m}^{-2}.\text{d}^{-1}$  in the NASW) is in agreement with data and satellite estimates. In the last province (NATR), the modelled PP ( $219 \text{ mgC.m}^{-2}.\text{d}^{-1}$ ) is slightly underestimated.

#### 4.4 DON at BATS and EUMELI stations

The dissolved organic nitrogen (DON) concentrations (the semi-labile fraction here) is underestimated in the simulation as compared to the BATS data (the difference between model and data averages (same definition as in Sec. 3.1) for the semi-labile DON is equal to  $-0.75 \text{ mmolN.m}^{-3}$ ) and EUMELI station ( $-1.45 \text{ mmolN.m}^{-3}$ ). The semi-labile DON pool is estimated by subtracting the refractory DON concentration (equal to  $2.45 \text{ mmolN.m}^{-3}$  at BATS station,  $3 \text{ mmolN.m}^{-3}$  at EUMELI station and

## Dissolved Organic Nitrogen and primary production

G. Charria et al.

2.14 mmolN.m<sup>-3</sup> along the AMT10 section) from the total DON measurement. The standard deviations for the simulated DON and DON data are quite comparable at BATS station (0.7 and 0.4 mmolN.m<sup>-3</sup>). At EUMELI station, the standard deviation is lower in the simulation (0.4 mmolN.m<sup>-3</sup>) as compared to the data (1 mmolN.m<sup>-3</sup>). At both stations, the correlation is low (less than 50%) due to the vertical structure of the simulated profile of DON as compared with the in situ DON profile. We also qualitatively compared the simulated DON section with the AMT10 (April–June 2000) section for DON concentrations. The range of concentrations is comparable, between 3 and 5 mmolN.m<sup>-3</sup> for the first 200 m depth.

### 5 Sensitivity studies for dissolved organic nitrogen

In order to assess the DON role in the North Atlantic Ocean (especially in the oligotrophic gyre), we perform parameter sensitivity analyses on a pre-bloom/bloom/post-bloom period from Mid-March to Mid-July 1998. We arbitrarily change the parameter values of the microbial loop in the simple biogeochemical model. Parameters are modified one by one and their reference values are: divided by two (–50%), multiplied by two (+100%) and equal to a very small value, 10<sup>-4</sup> (–100%) (Table 3). The model fields (DON, N, P, Z and D) are evaluated following the different experiments. The results are summarized using Taylor's representation.

This sensitivity study focuses on parameters related to the DON state variable. There are three sources of DON in the ecosystem model controlled by three parameters. First, a fraction of the phytoplankton exudation quantified by the  $\varepsilon$  coefficient is increasing the DON concentration. Another source is the dissolved organic part of the zooplankton excretion. This flux depends on two parameters, the zooplankton excretion ( $\gamma$ ) and the dissolved organic fraction of this excretion ( $f_2$ ). Finally, DON can increase through the hydrolysis process creating DON from particulate organic nitrogen. This last process is controlled by the hydrolysis rate coefficient ( $\mu_d$ ). The last parameter that we perturbed is the remineralization rate ( $\rho$ ), which represents the only DON

Title Page

Abstract

Introduction

Conclusions

References

Tables

Figures

◀

▶

◀

▶

Back

Close

Full Screen / Esc

Printer-friendly Version

Interactive Discussion



sink in our model (Fig. 1).

Figure 8 shows the results of these different experiments in terms of sensitivity to the surface concentrations. If we consider the  $\varepsilon$  parameter, it appears that it has a very weak influence on surface concentrations. The perturbed experiments have a strong correlation with the reference run and a standard deviation very close to the reference. The maximum concentration differences are under  $0.08 \text{ mmolN.m}^{-3}$  except for dissolved inorganic nitrogen in the Mauritanian upwelling, the subpolar gyre and the tropical regions where the differences reach  $0.25 \text{ mmolN.m}^{-3}$  (not shown). The zooplankton excretion flux, another source of DON, is driven by two parameters described above ( $\gamma$  and  $f_2$ ). Through the sensitivity experiments, the fraction  $f_2$  seems to have a weak effect on the N, Z, and DON concentrations (Fig. 8a, c, e). Correlations between sensitivity experiments and the reference simulation are high and standard deviations are similar. Surface concentration values remain almost unperturbed. At the opposite, the  $\gamma$  coefficient has no marked effect on N, Z and DON concentrations but the correlation is decreased as compared to the reference phytoplankton concentrations (Fig. 8b). Correlations are high for the phytoplankton concentrations, 0.99, but weaker than those obtained by these parameter changes on other state variables concentrations. Furthermore, the standard deviation of phytoplankton distribution decreases (increases) when the fluxes from Z to N are decreasing (increasing) (Fig. 8b). It shows a sensitivity of the phytoplankton standard deviation to the loss of dissolved inorganic nitrogen.

These two sources from the P and Z pools of DON (phytoplankton exudation and zooplankton excretion) do not have an impact on DON surface concentrations even if these fluxes are almost cancelled (Fig. 8e).

Results are different concerning the last and main source: the hydrolysis of particulate organic nitrogen. When this flux is nearly removed, the correlation ( $\sim 0.4$ ) dramatically decreases between the sensitivity experiment and the reference simulation for the DON concentrations and the standard deviation is divided by more than two (Fig. 8e). If we look at the concentration distribution, the subpolar gyre becomes depleted in DON except the eastern part of the basin between  $30^\circ \text{ N}$  and  $40^\circ \text{ N}$ . A similar impact is ob-

**Dissolved Organic Nitrogen and primary production**

G. Charria et al.

Title Page

Abstract

Introduction

Conclusions

References

Tables

Figures

◀

▶

◀

▶

Back

Close

Full Screen / Esc

Printer-friendly Version

Interactive Discussion



served in the tropical latitudes. More generally, concentrations dramatically decrease in the simulated field. This effect is also important when the flux is divided by a factor two. The inverse process, with an increase of surface concentrations, is occurring when the flux is doubled. These results show that the hydrolysis is the main source of DON in our area. The effect on other surface concentrations is similar except for nitrates, which tend to be less sensitive to the DON concentration (Fig. 8a). It can be explained by the overturning time, which is around 4 days from D to DON and around 40 days from DON to N in our simulation. Let's examine the sensitivity of the last component, sink of DON, and thus the concentrations sensitivity to the remineralization rate ( $\rho$ ). Even on this short time period (3.5 months), changes of the DON sink have a strong influence on surface concentrations. The main impact is observed on DON concentrations with a standard deviation very different from the reference simulation (Fig. 8e). The decrease in DON surface concentration can reach  $6 \text{ mmolN.m}^{-3}$  in the Mauritanian upwelling when the flux is stopped. Similar perturbations are observed on other state variables. For example, a strong effect can be noticed on phytoplankton concentrations in regions where the primary production is stronger (northern boundary of the subtropical gyre, Mauritanian upwelling and equator). In these regions, the concentration differences between the reference and the perturbed simulations reach  $0.6 \text{ mmolN.m}^{-3}$ . Perturbations of the remineralization rate have also an impact on dissolved inorganic nitrogen concentrations even if dissolved inorganic nitrogen from DON is quickly consumed. This effect is not clear following the statistics on the Taylor diagram (Fig. 8a) but the concentration increase and decrease are important (between 1 and  $3 \text{ mmolN.m}^{-3}$ ) in regions where nitrates concentrations are the highest (subpolar gyre, Mauritanian upwelling and equator) (not shown).

These sensitivity experiments showed that DON in the ecosystem model strongly depends on its main source: the hydrolysis. Other origins of DON have a weaker influence on other state variable concentrations in the model. As expected, the sink of DON, the remineralization loop between DON and N, has a significant effect on all model state variables. This analysis showed that DON plays an important role in less

## Dissolved Organic Nitrogen and primary production

G. Charria et al.

Title Page

Abstract

Introduction

Conclusions

References

Tables

Figures

◀

▶

◀

▶

Back

Close

Full Screen / Esc

Printer-friendly Version

Interactive Discussion



productive regions with respect to high productive regions (not shown), in agreement with the study from Gunson et al. (1999). Indeed, they showed that detrital sinking and remineralization rates have no influence on surface chlorophyll concentrations at high latitudes and great influence on surface chlorophyll concentrations at low latitudes.

## 6 Role of DON in sustaining primary production in the North Atlantic Ocean

We will examine here the source and sink terms as well as advection/diffusion of the N and DON equations to assess the DON role in sustaining the primary production in the oligotrophic region. We have shown in the previous section the central role of dissolved organic nitrogen (DON) in the North Atlantic Ocean. Let's discuss now the different nitrogen sources sustaining the primary production, especially the DON supply in the North Atlantic subtropical gyre. As examined by other studies (e.g., Mahaffey et al., 2004; Roussenov et al., 2006) based on modelling and/or in situ data, processes associated with DON dynamics could supply a part of the primary production in this oligotrophic gyre. Indeed, the lateral supply of DON from productive and upwelling zones might penetrate further into the subtropical gyre than does nitrate, because the semi-labile pool of DON has a longer lifetime in the euphotic zone (Williams and Follows, 1998).

The biological sources of inorganic nutrient simulated by the NPZDDON model, zooplankton excretion and remineralisation of DON by bacteria, are first examined. Over the subtropical gyre in the North Atlantic Ocean for the year 1998, the supply from DON (Fig. 9a) largely dominates the source from zooplankton excretion (Fig. 9b) by an order of magnitude. The northern and southern borders of the subtropical gyre as well as the large Mauritanian upwelling represent areas with large supply of inorganic nutrient:  $1.5\text{--}2\text{ molN.m}^{-2}.\text{yr}^{-1}$  from remineralisation of DON and  $0.2\text{--}0.3\text{ molN.m}^{-2}.\text{yr}^{-1}$  from zooplankton excretion (Fig. 9a, b). This general picture is consistent with the study from Williams and Follows (1998) and could be due to transport of DON from the enriched surrounding regions by the convergent Ekman transport over the subtropical

**BGD**

5, 1727–1764, 2008

## Dissolved Organic Nitrogen and primary production

G. Charria et al.

Title Page

Abstract

Introduction

Conclusions

References

Tables

Figures

◀

▶

◀

▶

Back

Close

Full Screen / Esc

Printer-friendly Version

Interactive Discussion



## Dissolved Organic Nitrogen and primary production

G. Charria et al.

Title Page

Abstract

Introduction

Conclusions

References

Tables

Figures

◀

▶

◀

▶

Back

Close

Full Screen / Esc

Printer-friendly Version

Interactive Discussion



gyre. This convergent transport can be decomposed in 3 main components: the off-shore transport of nutrient rich waters from the continental margins toward the centre of the subtropical gyre, the outward transport induced by the mean eastward wind at the northern boundary of the subtropical gyre as well as the northward transport induced by the trade winds at the southern flank of the subtropical gyre. We now examine the DON and inorganic nutrient supplies by physical transport, especially the meridional advection in the coupled model (Fig. 9c, d). As expected, the northern flank of the subtropical gyre represents a mean southward meridional transport of DON around  $-2.7 \text{ mmolN.m}^{-1}.\text{yr}^{-1}$  (around  $23^\circ \text{ N}$ ) and the southern flank a northward meridional advection around  $6.3 \text{ mmolN.m}^{-1}.\text{yr}^{-1}$  (around  $11.3^\circ \text{ N}$  – Fig. 9c).

The meridional transport of nitrate (Fig. 9d) differs from the transport of DON. The transport is higher than the transport of DON and it flows mainly southward south of  $25^\circ \text{ N}$  and northward between  $25^\circ \text{ N}$  and  $30^\circ \text{ N}$ .

To study the meridional supply of DON, the meridional transport of DON was zonally integrated over the basin from  $71^\circ \text{ W}$  to the eastern boundary (Fig. 10). From the wind field used to force the coupled model, the Ekman meridional flux of DON has also been estimated (Fig. 10). Between  $7^\circ \text{ N}$  and  $20^\circ \text{ N}$ , the total meridional DON transport is northward as well as the Ekman component. However, the total component is smaller than the Ekman contribution. At the opposite, between  $22^\circ \text{ N}$  and  $36^\circ \text{ N}$ , the total southward DON transport has mainly a reverse direction as compared to the Ekman component. In between ( $20^\circ \text{ N}$ – $22^\circ \text{ N}$ ), the total DON transport is close to zero. This area is associated with the lowest primary production value in the subtropical gyre. Other processes, as meridional current components, eddies, meanders and fronts, decrease the northward DON transport mainly driven by the Ekman dynamics. Furthermore, the difference between the Ekman transport and the total transport, reaching  $+10.7 \text{ kmolN.s}^{-1}$  (Fig. 10), has a stronger influence north of  $22^\circ \text{ N}$ . Indeed, it induces a change in the transport direction. The meridional DON supply in the subtropical gyre of the North Atlantic Ocean can not be systematically explained only by the Ekman dynamics. Indeed, the southward total transport at the northern border

of the subtropical gyre is mainly driven by other processes. Our estimates, using a realistic modelling approach, are in agreement with previous studies using simplified cycling and transport model for DON and in situ data. For example, Roussenov et al. (2006) found a  $179 \text{ kmolN.s}^{-1}$  at  $12^\circ \text{ N}$  of meridional flux of total DON. Assuming a 10% fraction of semi-labile DON in the total DON (as in Mahaffey et al., 2004), this estimation ( $17.9 \text{ kmolN.s}^{-1}$ ) compares quite well with our meridional modelled transport of  $18 \text{ kmolN.s}^{-1}$ . Mahaffey et al. (2004) found an Ekman northward semi-labile DON flux equal to  $0.5 \text{ mmolN.m}^{-1}.\text{s}^{-1}$  along the AMT10 transect at  $10^\circ \text{ N}$ ,  $21.5^\circ \text{ W}$ . This estimation is very similar to the value of  $0.65 \text{ mmolN.m}^{-1}.\text{s}^{-1}$  at the same location obtained from our simulations. Assuming the same approximation than in Mahaffey et al. (2004) (same value of meridional DON transport over a 4000-km zonal band at  $10^\circ \text{ N}$ ), we found a  $2.6 \text{ kmolN.s}^{-1}$  for the meridional semi-labile DON transport. This value is comparable to the  $2.0 \text{ kmolN.s}^{-1}$  value ( $0.5 \text{ mmolN.m}^{-1}.\text{s}^{-1} \times 4000 \text{ km}$ ) from Mahaffey et al. (2004). These estimations are much lower than the zonally integrated value ( $19.4 \text{ kmolN.s}^{-1}$ ) at  $10^\circ \text{ N}$  (Fig. 10). The heterogeneous zonal distribution of the meridional DON transport represents an important factor to take into account for the estimation of the zonally integrated meridional DON flux.

Our analyses showed that the DON supply in the subtropical gyre is mainly driven by the meridional Ekman transport, south of  $20^\circ \text{ N}$ , as suggested in recent studies (Mahaffey et al., 2004; Roussenov et al., 2006). However, our study pointed out the contribution of other processes (meridional current components, eddies, meanders and fronts) mainly in the northern part of the subtropical gyre.

To identify the processes sustaining primary production and to compare the different sources-sinks of nitrate and DON, an upper water column budget for these two quantities was computed in the first 112 m depth over a given area in the subtropical gyre (between  $13^\circ$  and  $35^\circ \text{ N}$  and between  $71$  and  $40^\circ \text{ W}$  – Fig. 9b) for the year 1998 (Fig. 11). The primary production is in good agreement with other estimations (see Table 2) and it corresponds to  $756 \cdot 10^{13} \text{ mmolN}$  over the budget area. This primary production is mainly sustained by biological nitrogen supply from zooplankton excretion

## Dissolved Organic Nitrogen and primary production

G. Charria et al.

Title Page

Abstract

Introduction

Conclusions

References

Tables

Figures

◀

▶

◀

▶

Back

Close

Full Screen / Esc

Printer-friendly Version

Interactive Discussion



and DON remineralisation (99%;  $751 \cdot 10^{13}$  mmolN). The Dissolved Inorganic Nitrogen (DIN) necessary to sustain this primary production comes mainly from the DON pool. It represents 85% of the DIN biological sources. If we investigate further the origins of the DIN available for primary production, we can notice that the main source of the DON supply by advection is the meridional transport of DON (80%,  $27.7 \cdot 10^{13}$  mmolN). The other sources of DON come from the exudation of phytoplankton, organic excretion of zooplankton and hydrolysis of particulate organic nitrogen.

Following the biogeochemical fluxes in this region (Fig. 11), it appears clearly that the meridional advection of DON is an important source of DIN necessary to sustain primary production. However, the advection and diffusion of DIN also represent a small source of nitrogen ( $17.3 \cdot 10^{13}$  mmolN) which could be much more important if it was not balanced by a loss of nitrogen by vertical advection.

The dissolved organic matter plays a key role in nitrogen, but also in phosphorus cycling. For example, at BATS (Salihoglu et al., 2008) and at HOT in the North Pacific subtropical gyre (Christian, 2005), the importance of the Dissolved Organic Phosphorus (DOP) has been demonstrated using modelling and in situ measurements. The DOP can sustain the level of primary production in these nitrogen and phosphorus limited regions. Indeed, studies in the last ten years have highlighted the role of phosphorus as a limiting nutrient in the Atlantic Ocean (Wu et al., 2000; Lipschultz et al., 2002; Ammerman et al., 2003; Lomas et al., 2004). Furthermore, in the present study, a fixed C/N ratio was used to estimate the C-based primary production. However, limiting nutrients depend on C/N/P ratio, which can be different of the canonical Redfield ratio. For example, Christian (2005) and Salihoglu et al. (2008) obtained a better estimation of the primary production using variable intracellular C/N/P for phytoplankton. Indeed, the decrease of the primary production with depth is well reproduced in agreement with in situ data.

In summary, the DON represents an important source of DIN in the subtropical gyre of the North Atlantic Ocean. The supply of DON by physical processes in this gyre is dominated by meridional transports. Indeed, south of  $20^{\circ}$  N, a northern transport

**Dissolved Organic Nitrogen and primary production**

G. Charria et al.

Title Page

Abstract

Introduction

Conclusions

References

Tables

Figures

◀

▶

◀

▶

Back

Close

Full Screen / Esc

Printer-friendly Version

Interactive Discussion



mainly due to the Ekman component sustains the primary production in the oligotrophic gyre. This input is increased by a southward transport north of 22° N associated with non-Ekman dynamics. Our estimate of the mean value of the meridional DON transport,  $0.039 \text{ molN.m}^{-2}.\text{yr}^{-1}$ , confirms the importance of this process as compared to other possible mechanisms, ranging from 0.05 to  $0.07 \text{ molN.m}^{-2}.\text{yr}^{-1}$ , to fuel primary production in the North Atlantic subtropical gyre. The dissolved organic nitrogen and phosphorus, and the variable C/N/P for phytoplankton should be implemented in a three-dimensional view of the North Atlantic Ocean. To fully understand the processes controlling primary and export productions as well as the climate change impact on the ocean, the phosphorus cycle should be considered as well as other cycles (silicon and iron).

*Acknowledgements.* Financial support for this work was provided by the GMMC (Groupe Mission MERCATOR/CORIOLIS) to I. Dadou and V. Garçon at LEGOS (Toulouse, France). The physical model was provided by MERCATOR (<http://www.mercator-ocean.fr>). The calculations were conducted with the support of IDRIS/CNRS. The work was funded by CNES and IFREMER through a PhD fellowship, by the University Paul Sabatier through a postdoctoral fellowship and by the European Commission through a Marie-Curie postdoctoral fellowship. We are grateful to the AMT project (C. Robinson) for providing their data and C. Mahaffey for useful discussions.

## References

- Aiken, J. and Bale, A. J.: An introduction to the Atlantic Meridional Transect (AMT) programme, Prog. Oceanogr., 45, 251–256, 2000.
- Ammerman, J. W., Hood, R. R., Case, D. A., and Cotner, J. B.: Phosphorus deficiency in the Atlantic: An emerging paradigm in oceanography, EOS, 84, 165–170, 2003.
- Antoine, D., and Morel, A.: Ocean Primary Production, 2: Estimation at global scale from satellite (Coastal Zone Color Scanner) chlorophyll, Global Biogeochem. Cy., 10, 57-69, 1996.
- Barnier, B., Miranda, A., Crosnier, L., Molines, J.-M., Tréguier A.-M., and Jouzeau, A.: Rapport scientifique et technique 1999, N°CLIPPER-R3-2000, LPO, Brest, 2000.

**BGD**

5, 1727–1764, 2008

## Dissolved Organic Nitrogen and primary production

G. Charria et al.

Title Page

Abstract

Introduction

Conclusions

References

Tables

Figures

◀

▶

◀

▶

Back

Close

Full Screen / Esc

Printer-friendly Version

Interactive Discussion



- Barnier, B., Madec, G., Penduff, T., Molines, J.-M., Tréguier, A.-M., Le Sommer, J., Beckmann, A., Biastoch, A., Böning, C., Dengg, J., Derval, C., Durand, E., Gulev, S., Remy, E., Talandier, C., Theetten, S., Maltrud, M., McClean, J., and De Cuevas, B.: Impact of partial steps and momentum advection schemes in a global ocean circulation model at eddy-permitting resolution, *Ocean Dynam.*, 56, 543–567, 2006.
- Behrenfeld, M. J. and Falkowski, P.: Photosynthetic rates derived from satellite-based chlorophyll concentration, *Limnol. Oceanogr.*, 42, 1–20, 1997.
- Berline L., Brankart, J. M., Brasseur, P., Ourmières, Y., and Verron, J.: Improving the physics of a coupled physical-biogeochemical model of the North Atlantic through data assimilation: Impact on the ecosystem, *J. Marine Syst.*, 64 (1-4), 153–172, 2007.
- Blanke, B. and Delecluse, P.: Variability of the tropical Atlantic ocean simulated by a general circulation model with two different mixed-layer physics, *J. Phys. Oceanogr.*, 23, 1363–1388, 1993.
- Carr M. E., Friedrichs, M. A. M., Schmeltz, M., et al.: A comparison of global estimates of marine primary production from ocean color, *Deep-Sea Res. Pt II*, 53(5–7), 741–770, 2006.
- Charria, G.: Influence of Rossby waves on the biogeochemical system in the North Atlantic Ocean: Use of ocean colour remotely sensed data and of a coupled physical/biogeochemical model, PhD Thesis, University Paul Sabatier, Toulouse, France, 339 pp., 2005.
- Christian, J. R.: Biogeochemical cycling in the oligotrophic ocean: Redfield and non-Redfield models. *Limnol. Oceanogr.*, 50(2), 646–657, 2005.
- Conkright, M., O'Brien, T., Levitus, S., Boyer, T. P., Antonov, J., and Stephens, C.: *World Ocean Atlas 1998*, NOAA Atlas NESDIS 36. US Gov. Printing Office, Wash., D. C., 245 pp., 1998.
- Drillet, Y., Bourdalle-Badie, R., Siefridt, L., and Le Provost, C.: Meddies in the Mercator North Atlantic and Mediterranean sea eddy resolving model, *J. Geophys. Res.*, 110, C03016, doi:10.1029/2003JC002170, 2005.
- Ducklow, H. W.: Biogeochemical Provinces: Towards a JGOFS Synthesis, in: *Ocean Biogeochemistry*, edited by: M. J. R. Fasham, Springer Verlag, 3–17, 2003.
- Emerson, S., Quay, P., Karl, D., Winn, C., Tupas, L., and Landry, M.: Experimental determination of the organic carbon flux from open-ocean surface waters, *Nature*, 389(6654), 951–954, 1997.
- Estubier, A. and Lévy, M.: Quel schéma numérique pour le transport d'organismes biologiques par la circulation océanique? Note Technique du Pôle de modélisation, Institut Pierre-Simon Laplace (IPSL), 81 pp., 2000.

---

## Dissolved Organic Nitrogen and primary production

G. Charria et al.

---

Title Page

Abstract

Introduction

Conclusions

References

Tables

Figures

◀

▶

◀

▶

Back

Close

Full Screen / Esc

Printer-friendly Version

Interactive Discussion



- Gruber, N. and Sarmiento, J. L.: Global patterns of marine nitrogen fixation and denitrification, *Global Biogeochem. Cy.*, 11(2), 235–266, 1997.
- Gunson, J., Oschlies, A., and Garçon, V.: Sensitivity of ecosystem parameters to simulated satellite ocean colour data using a coupled physical-biological model of the North Atlantic, *J. Mar. Res.*, 57, 613–639, 1999.
- Hansell, D. A., Ducklow, H. W., Macdonald, A. M., and Baringer, M. O.: Metabolic poise in the North Atlantic Ocean diagnosed from organic matter transports, *Limnol. Oceanogr.*, 49(4), 1084–1094, 2004.
- Huret, M., Dadou, I., Dumas, F., Lazure, P., and Garçon, V.: Coupling physical and biogeochemical processes in the Río de la Plata plume, *Cont. Shelf Res.*, 25, 629–653, 2005.
- Huret, M.: Apport des données satellitales de la couleur de l'eau à la modélisation couplée physique-biogéochimie en milieu dynamique côtier : Application au Río de la Plata et au Golfe de Gascogne, PhD Thesis, University Paul Sabatier, Toulouse, France, 274 pp., 2005.
- Lipschultz, F., Bates, N., Carlson, C., and Hansell, D.: New production in the Sargasso Sea: History and current status. *Global Biogeochem. Cy.*, 16, 1–16, 2002.
- Lomas, M. W. and Bates, N. R.: Potential controls on interannual partitioning of organic carbon during the winter/spring phytoplankton bloom at the Bermuda Atlantic Time-series (BATS) site, *Deep-Sea Res. Pt I*, 51, 1619–1636, 2004.
- Longhurst, A.: *Ecological Geography of the Sea*, Academic Press, 542 pp., 1998.
- McClain, C. R., Signorini, S. R., and Christian, J. R.: Subtropical gyre variability observed by ocean-color satellites, *Deep-Sea Res. Pt II*, 51, 281–301, 2004.
- McGillicuddy, D. J. and Robinson, A. R.: Eddy-induced nutrient supply and new production in the Sargasso Sea, *Deep-Sea Res. Pt I*, 44(8), 1427–1450, 1997.
- Madec, G., Delecluse, P., Imbard, M., and Levy, C.: OPA 8.1 Ocean General Circulation Model reference manual, Note Technique du Pôle de modélisation, Institut Pierre-Simon Laplace (IPSL), France, 91 pp., 1999.
- Mahaffey, C., Williams, R. G., Wolff, G. A., and Anderson, W.: Physical supply of nitrogen to phytoplankton in the Atlantic Ocean, *Global Biogeochem. Cy.*, 18, GB1034, doi:10.1029/2003GB002129, 2004.
- Mélin, F.: Potentiel de la télédétection pour l'analyse des propriétés optiques du système océan-atmosphère et application à l'estimation de la photosynthèse phytoplantonique, PhD Thesis, University Paul Sabatier, Toulouse, 514 pp., 2003.
- Morel, A., Antoine, D., Babin, M., and Dandonneau, Y.: Measured and modeled primary pro-

---

## Dissolved Organic Nitrogen and primary production

G. Charria et al.

---

Title Page

Abstract

Introduction

Conclusions

References

Tables

Figures

◀

▶

◀

▶

Back

Close

Full Screen / Esc

Printer-friendly Version

Interactive Discussion



duction in the northeast Atlantic (EUMELI JGOFS program): The impact of natural variations in photosynthetic parameters on model predictive skill, *Deep-Sea Res. Pt I*, 43 (8), 1273–1304, 1996.

O'Reilly, J. E., S. Maritorena, D. A. Siegel, et al.: Ocean Color Chlorophyll *a* Algorithms for SeaWiFS, OC2, and OC4: Version 4, SeaWiFS Postlaunch Calibration and Validation Analyses, Part 3, NASA Technical Memorandum 206892, 11, 923, 2000.

Oschlies, A.: Can eddies make ocean deserts bloom?, *Global Biogeochem. Cy.*, 16(4), 1106, doi: 10.1029/2001GB001830, 2002.

Oschlies, A., and Garçon, V.: An eddy-permitting coupled physical-biological model of the North Atlantic. 1. Sensitivity to advection numerics and mixed layer physics, *Global Biogeochem. Cy.*, 13(1), 135–160, 1999.

Palter, J. B., Lozier, M. S., and Barber, R. T.: The effect of advection on the nutrient reservoir in the North Atlantic subtropical gyre, *Nature*, 437,687–692, 2005.

Reynaud, T., Legrand, P., Mercier, H., and Barnier, B.: A new analysis of hydrographic data in the Atlantic and its application to an inverse modelling study, *International WOCE Newsletters*, 32, 1998.

Reynolds, R. W. and Smith, T.: Improved global sea surface temperature analysis using optimum interpolation, *J. Climate*, 7, 929–948, 1994.

Roussenov, V., Williams, R. G., Mahaffey, C., and Wolff, G. A.: Does the transport of dissolved organic nutrients affect production in the Atlantic Ocean?, *Global Biogeochem. Cy.*, 20, GB3002, doi:10.1029/2005GB002510, 2006.

Salihoglu, B., Garçon, V., Oschlies, A., and Lomas, M. W.: Influence of nutrient utilization and remineralization stoichiometry on phytoplankton species and carbon export: a modeling study at BATS, *Deep-Sea Res. Pt I*, 55, 73–107, 2008.

Sarmiento, J. L., Slater, R. D., Fasham, M. J. R., Ducklow, H. W., Toggweiler, J. R., and Evans, G. T.: A Seasonal Three-Dimensional Ecosystem Model of Nitrogen Cycling in the North Atlantic Euphotic Zone, *Global Biogeochem. Cy.*, 7(2), 417–450, 1993.

Siegel, D. A., McGillicuddy, D. J. Jr., and Fields, E. A.: Mesoscale eddies, satellite altimetry, and new production in the Sargasso Sea, *J. Geophys. Res.*, 104(C6), 13 359–13 379, 1999.

Steinberg, D. K., Carlson, C. A., Bates, N. R., Johnson, R. J., Michaels, A. F., and Knap, A. H.: Overview of the US JGOFS Bermuda Atlantic Time-series Study (BATS): a decade-scale look at ocean biology and biogeochemistry, *Deep-Sea Res. Pt II*, 48, 1405–1447, 2001.

Taylor, K. E.: Summarizing multiple aspects of model performance in a single diagram, *J.*

**BGD**

5, 1727–1764, 2008

---

## Dissolved Organic Nitrogen and primary production

G. Charria et al.

---

Title Page

Abstract

Introduction

Conclusions

References

Tables

Figures

◀

▶

◀

▶

Back

Close

Full Screen / Esc

Printer-friendly Version

Interactive Discussion



Geophys. Res., 106(D7), 7183–7192, 2001.

Tréguier, A. M., Barnier, B., de Miranda, A., Molines, J.-M., Grima, N., Imbard, M., Madec, G., Messenger, C., and Michel, S.: An eddy permitting model of the Atlantic circulation: evaluating open boundary conditions, *J. Geophys. Res.*, 106, 22 115–22 129, 2001.

5 Williams, G. G. and Follows, M. J.: The Ekman transfer of nutrients and maintenance of new production over the North Atlantic, *Deep-Sea Res. Pt I*, 45 (2–3), 461–489, 1998.

Wu, J., Sunda, W., Boyle, E. A., and Karl, D. M.: Phosphate depletion in the western North Atlantic Ocean, *Science*, 289, 759–762, 2000.

**BGD**

5, 1727–1764, 2008

---

## Dissolved Organic Nitrogen and primary production

G. Charria et al.

---

Title Page

Abstract

Introduction

Conclusions

References

Tables

Figures

◀

▶

◀

▶

Back

Close

Full Screen / Esc

Printer-friendly Version

Interactive Discussion



**Dissolved Organic Nitrogen and primary production**

G. Charria et al.

Title Page

Abstract

Introduction

Conclusions

References

Tables

Figures

◀

▶

◀

▶

Back

Close

Full Screen / Esc

Printer-friendly Version

Interactive Discussion



**Table 1.** Parameters of the biogeochemical model.

Parameter	Symbol	Value	Units
Initial slope of P-I curve	$\alpha$	0.025	$(\text{W}\cdot\text{m}^{-2})^{-1}\text{d}^{-1}$
Photosynthetically active radiation	PAR	0.43	–
Light attenuation coefficient of pure water	$k_w$	0.04	$\text{m}^{-1}$
Light attenuation coefficient of chlorophyll	$k_c$	0.03	$\text{m}^{-1}(\text{mmol}\cdot\text{m}^{-3})^{-1}$
Maximum growth rate parameters	$a$	0.6	$\text{d}^{-1}$
	$b$	1.066	–
	$c$	1	$(^\circ)^{-1}$
Half saturation concentration for nutrient uptake	$K_N$	0.5	$\text{mmolN}\cdot\text{m}^{-3}$
Phytoplankton mortality rate	$\lambda_P$	0.03	$\text{d}^{-1}$
Phytoplankton exudation rate	$\varepsilon$	0.01	–
Assimilation efficiency of zooplankton	$f_1$	0.75	–
Maximum zooplankton grazing rate	$g$	2	$\text{d}^{-1}$
Zooplankton capture rate	P	1	$(\text{mmol}\cdot\text{m}^{-3})^{-2}\text{d}^{-1}$
(Quadratic) zooplankton mortality	$\lambda_Z$	0.2	$(\text{mmolN}\cdot\text{m}^{-3})^{-1}\text{d}^{-1}$
Zooplankton excretion rate	$\gamma$	0.03	$\text{d}^{-1}$
Organic fraction of excretion	$f_2$	0.25	–
Hydrolysis rate of detritus	$\mu_D$	0.23	$\text{d}^{-1}$
Sinking velocity	$V_D$	5	$\text{m}\cdot\text{d}^{-1}$
Remineralization rate	$\rho$	0.025	$\text{d}^{-1}$

Dissolved Organic Nitrogen and primary production

G. Charria et al.

**Table 2.** Primary production ( $\text{mgC}\cdot\text{m}^{-2}\cdot\text{d}^{-1}$ ) estimated by different studies (this study, JGOFS (Ducklow, 2003), ME (Mélin, 2003), AM96 (Antoine and Morel, 1996) and BF97 (Behrenfeld and Falkowski, 1997) for different biogeochemical provinces as defined by Longhurst (1998): ARCT (Atlantic Arctic Province), SARC (Atlantic Subarctic Province), NADR (North Atlantic Subtropical Drift Province), GFST (Gulf Stream province), NASW (North Atlantic Subtropical Gyral Province – West), NASE (North Atlantic Subtropical Gyral Province – East), NATR (North Atlantic Tropical Gyre Province) see Sect. 3.3 for details.

Biogeochemical provinces	JGOFS	ME	AM96	BF 97	This study
ARCT	1330	507	430	687	173
SARC	830	472	483	887	249
NADR	660	555	484	852	230
GFST	490	522	488	677	363
NASW	459	304	355	360	448
NASE	330	410	413	526	392
NATR	290	313	513	363	219

Title Page

Abstract

Introduction

Conclusions

References

Tables

Figures

◀

▶

◀

▶

Back

Close

Full Screen / Esc

Printer-friendly Version

Interactive Discussion



**Dissolved Organic Nitrogen and primary production**

G. Charria et al.

**Table 3.** Parameters value during sensitivity experiments for  $\varepsilon$ ,  $f_2$ ,  $\gamma$ ,  $\mu_d$ ,  $\rho$ .

Parameter	Reference	+ 100%	-50%	-100%
$\varepsilon$	0.01	0.02	0.005	$10^{-4}$
$f_2$	0.25	0.5	0.125	$10^{-4}$
$\gamma$	$0.03 \text{ d}^{-1}$	$0.06 \text{ d}^{-1}$	$0.015 \text{ d}^{-1}$	$10^{-4} \text{ d}^{-1}$
$\mu_d$	$0.23 \text{ d}^{-1}$	$0.46 \text{ d}^{-1}$	$0.115 \text{ d}^{-1}$	$10^{-4} \text{ d}^{-1}$
$\rho$	$0.025 \text{ d}^{-1}$	$0.05 \text{ d}^{-1}$	$0.0125 \text{ d}^{-1}$	$10^{-4} \text{ d}^{-1}$

Title Page

Abstract

Introduction

Conclusions

References

Tables

Figures



Back

Close

Full Screen / Esc

Printer-friendly Version

Interactive Discussion



Dissolved Organic Nitrogen and primary production

G. Charria et al.

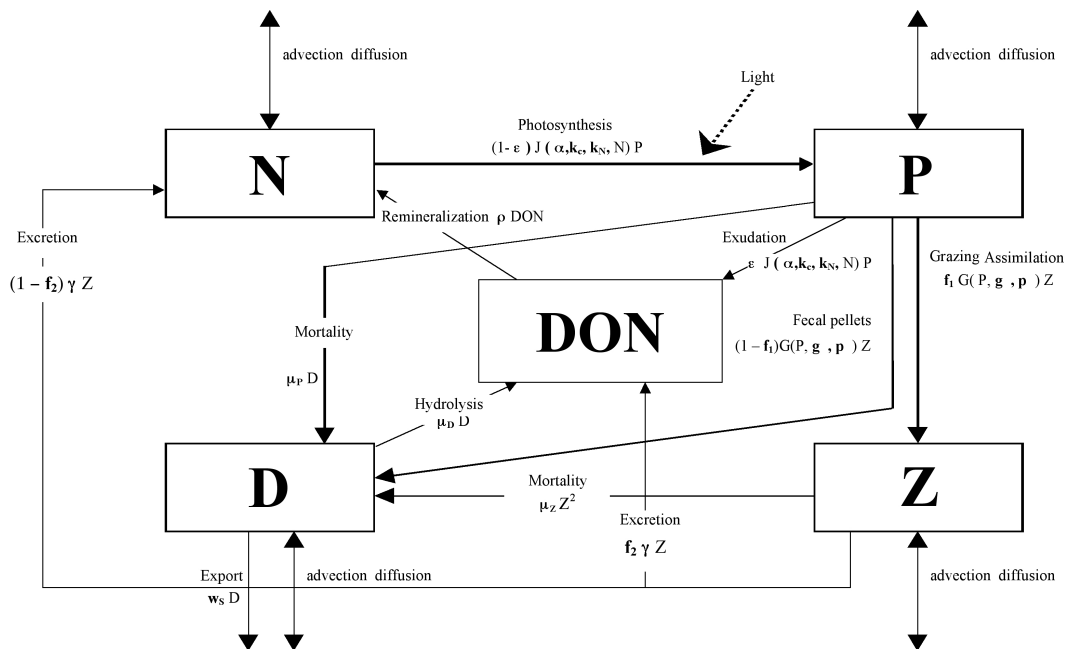


Fig. 1. The biogeochemical model from Huret et al. (2005).

Title Page	
Abstract	Introduction
Conclusions	References
Tables	Figures
◀	▶
◀	▶
Back	Close
Full Screen / Esc	
Printer-friendly Version	
Interactive Discussion	



Dissolved Organic Nitrogen and primary production

G. Charria et al.

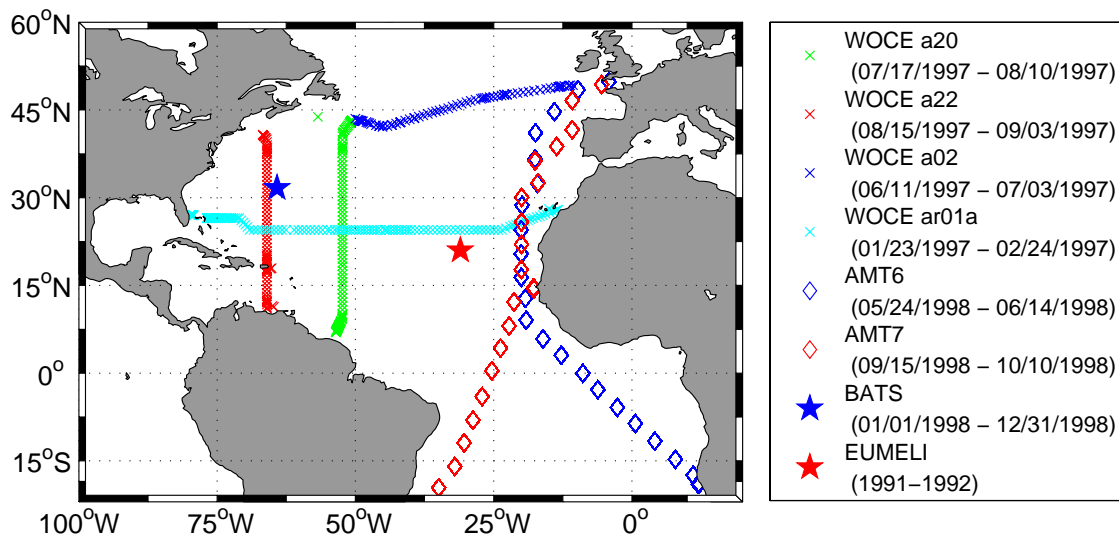


Fig. 2. Sections and stations used for the model/data comparison (latitude, longitude, time period and data).

Title Page

Abstract Introduction

Conclusions References

Tables Figures

◀ ▶

◀ ▶

Back Close

Full Screen / Esc

Printer-friendly Version

Interactive Discussion



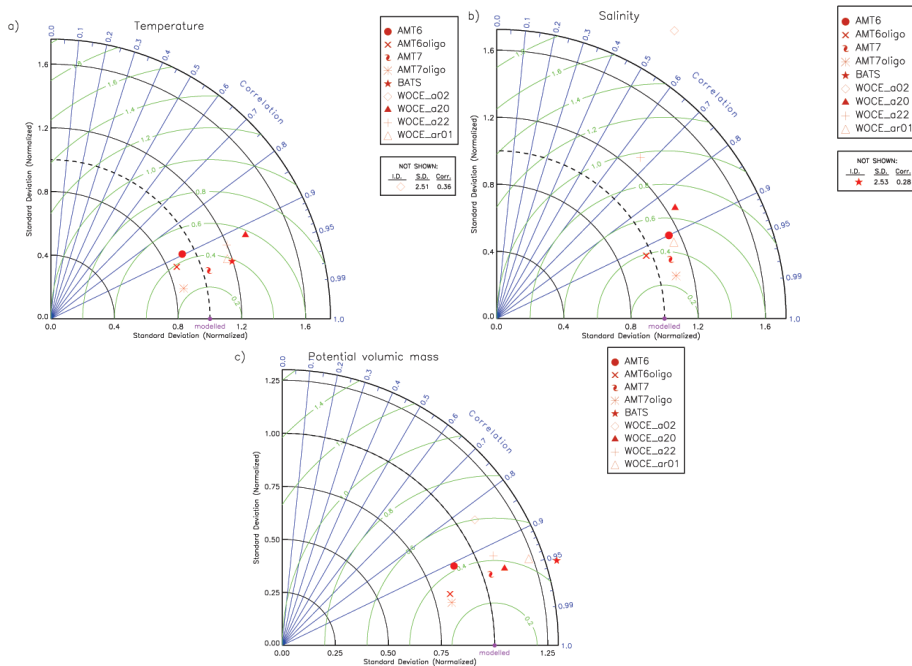


**Fig. 3.** Model performance analyses using Taylor's diagrams for **(a)** Temperature, **(b)** Salinity and **(c)** Density. The radial distance from the origin is proportional to the standard deviation of a pattern (normalised by the modelled standard deviation). The centred root mean square difference between the modelled and data fields (green line) is proportional to their distance apart (normalised). The correlation between the two fields is given by the azimuthal position of the test field. I.D., S.D., Corr stand for the symbol identifier, the standard deviation and the correlation, respectively. As it is mentioned in Sect. 3, the statistical metrics were computed following the available data for each dataset (vertical sections, time series or surface fields). Abbreviations used are: AMT6- AMT6 section (May–June 1998), AMT6 oligo- AMT6 section only in the oligotrophic gyre, AMT7-AMT7 section (September–October 1998), AMT7 oligo-AMT7 section only in the oligotrophic gyre, BATS-Bermuda Atlantic Time-series Study (January–December 1998), WOCE\_a02-WOCE section a02 (June–July 1997), WOCE\_a20-WOCE section a20 (July–August 1997), WOCE\_a22-WOCE section a22 (August–September 1997), WOCE\_ar01-WOCE section ar01 (January–February 1998).

Title Page

Abstract

Introduction

Conclusions

References

Tables

Figures

◀

▶

◀

▶

Back

Close

Full Screen / Esc

Printer-friendly Version

Interactive Discussion



Dissolved Organic Nitrogen and primary production

G. Charria et al.

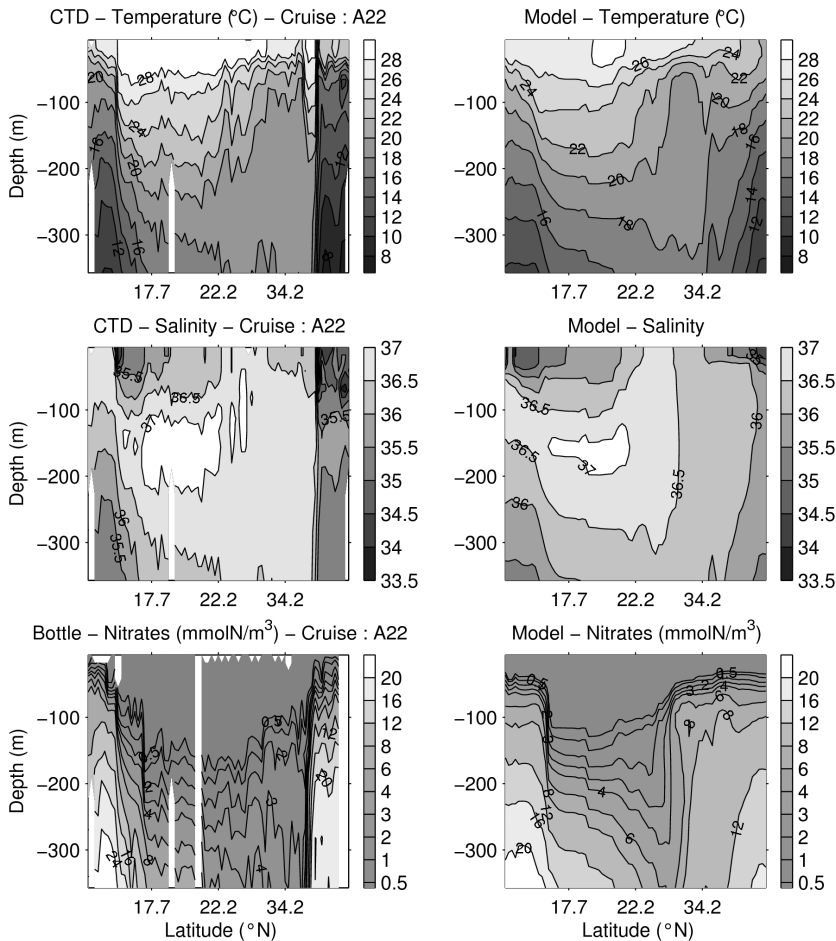


**Fig. 4.** Temperature (top), Salinity (middle), and Nitrates (bottom) measured along the WOCE A22 transect (left) and estimated with the coupled model (right) for the first 350 m depth.

Title Page

Abstract Introduction

Conclusions References

Tables Figures

◀ ▶

◀ ▶

Back Close

Full Screen / Esc

Printer-friendly Version

Interactive Discussion



Dissolved Organic  
Nitrogen and primary  
production

G. Charria et al.

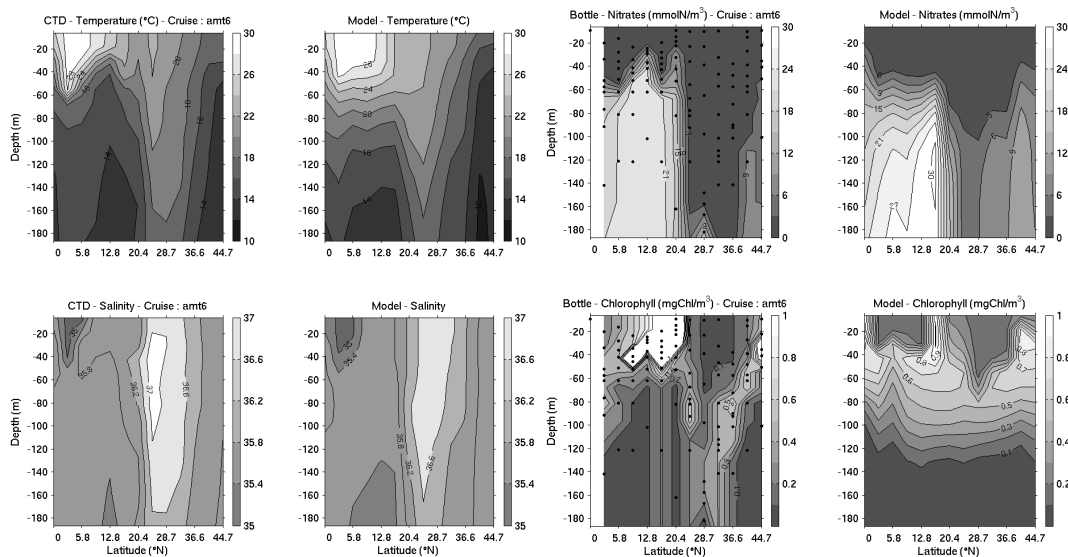


**Fig. 5.** (a) Temperature (top) and Salinity (bottom) measured along the AMT6 transect (left) and estimated with the coupled model (right) for the first 200 m depth.  
 (b) Nitrates (top) and Chlorophyll (bottom) measured along the AMT6 transect and estimated with the coupled model (right) for the first 200 m depth.

Title Page

Abstract

Introduction

Conclusions

References

Tables

Figures

◀

▶

◀

▶

Back

Close

Full Screen / Esc

Printer-friendly Version

Interactive Discussion



Dissolved Organic Nitrogen and primary production

G. Charria et al.

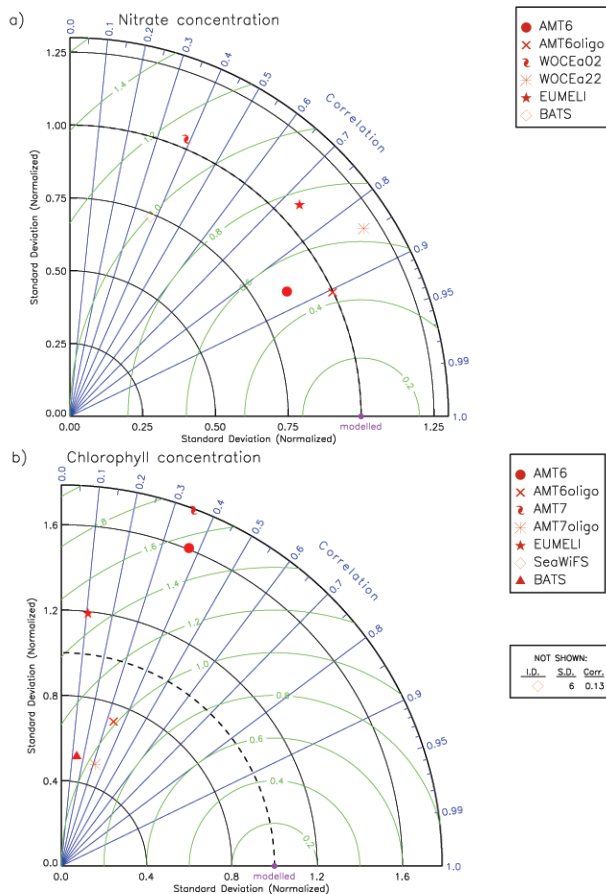


**Fig. 6.** Model performance analyses using Taylor’s diagrams for **(a)** nitrates and **(b)** chlorophyll surface concentrations. EUMELI stands for EUMELI data (1991–1992) at 21° N and 31° W. SeaWiFS stands for the year 1998 over the model domain. See the legend of Fig. 2 for details and other abbreviations.

Title Page

Abstract Introduction

Conclusions References

Tables Figures

◀ ▶

◀ ▶

Back Close

Full Screen / Esc

Printer-friendly Version

Interactive Discussion



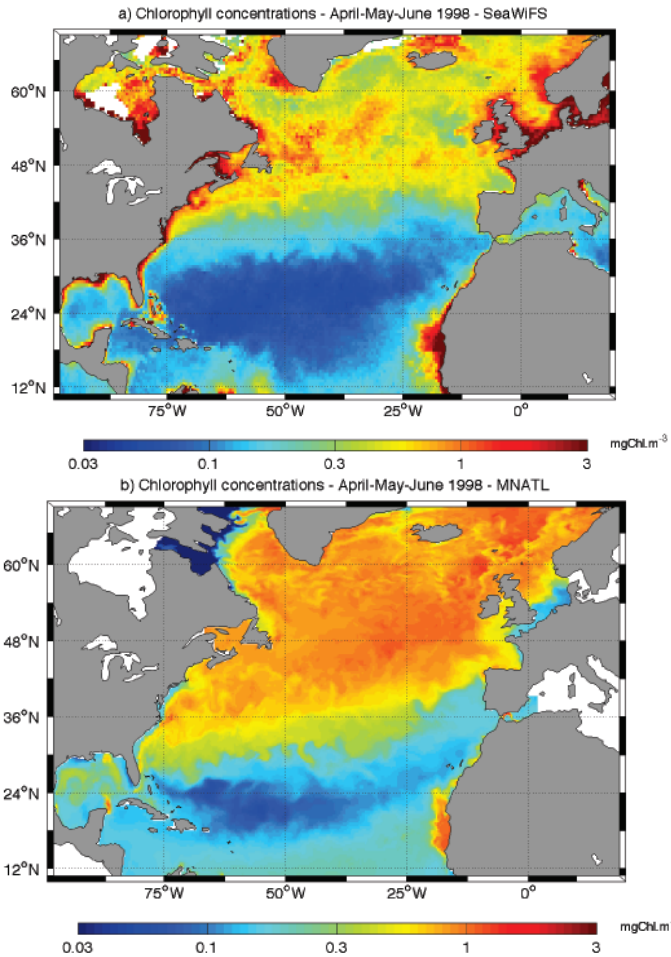


**Fig. 7.** Surface Chlorophyll concentration ( $\text{mgChl.m}^{-3}$ ) averaged from April up to June 1998 with **(a)** SeaWiFS data and with **(b)** the coupled modelled fields.

**BGD**

5, 1727–1764, 2008

## Dissolved Organic Nitrogen and primary production

G. Charria et al.

Title Page

Abstract

Introduction

Conclusions

References

Tables

Figures

◀

▶

◀

▶

Back

Close

Full Screen / Esc

Printer-friendly Version

Interactive Discussion



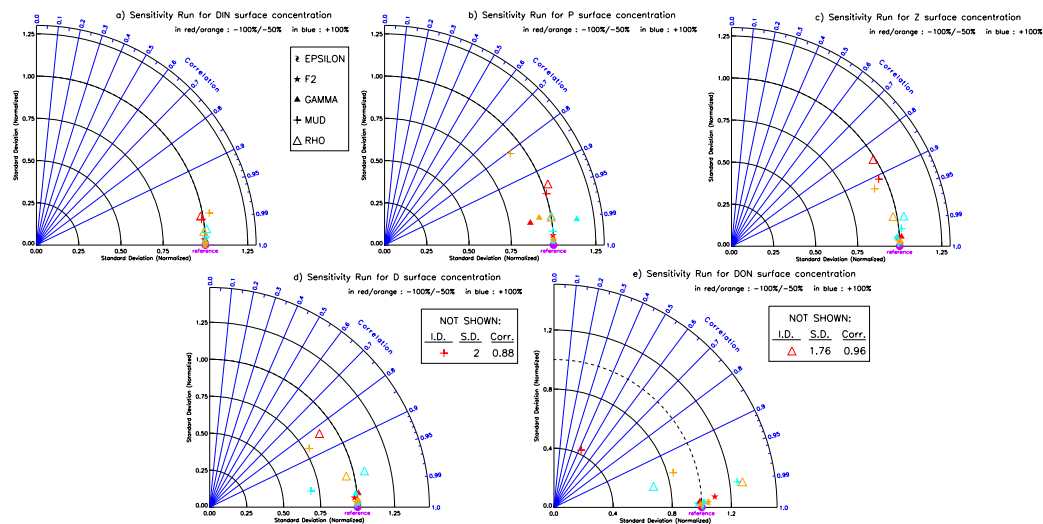


**Fig. 8.** Model performance analyses using Taylor's diagrams showing results of sensitivity experiments (from mid-March to mid-July 1998, over the model domain) on surface Dissolved inorganic nitrogen **(a)**, Phytoplankton **(b)**, Zooplankton **(c)**, Particulate organic nitrogen **(d)** and Dissolved organic nitrogen **(e)** over the whole basin. The radial distance from the origin is proportional to the standard deviation of a pattern (normalised by the standard deviation of the simulation of reference). The correlation between the two fields, the simulation of reference and the simulation with the modified parameter value, is given by the azimuthal position of the test field.  $\epsilon$ ,  $f_2$ ,  $\gamma$ ,  $\mu_d$  and  $\rho$  represent phytoplankton exudation rate, organic fraction of excretion, zooplankton excretion rate, hydrolysis rate of detritus and remineralisation rate, respectively.

## Dissolved Organic Nitrogen and primary production

G. Charria et al.

Title Page

Abstract

Introduction

Conclusions

References

Tables

Figures

◀

▶

◀

▶

Back

Close

Full Screen / Esc

Printer-friendly Version

Interactive Discussion



## Dissolved Organic Nitrogen and primary production

G. Charria et al.

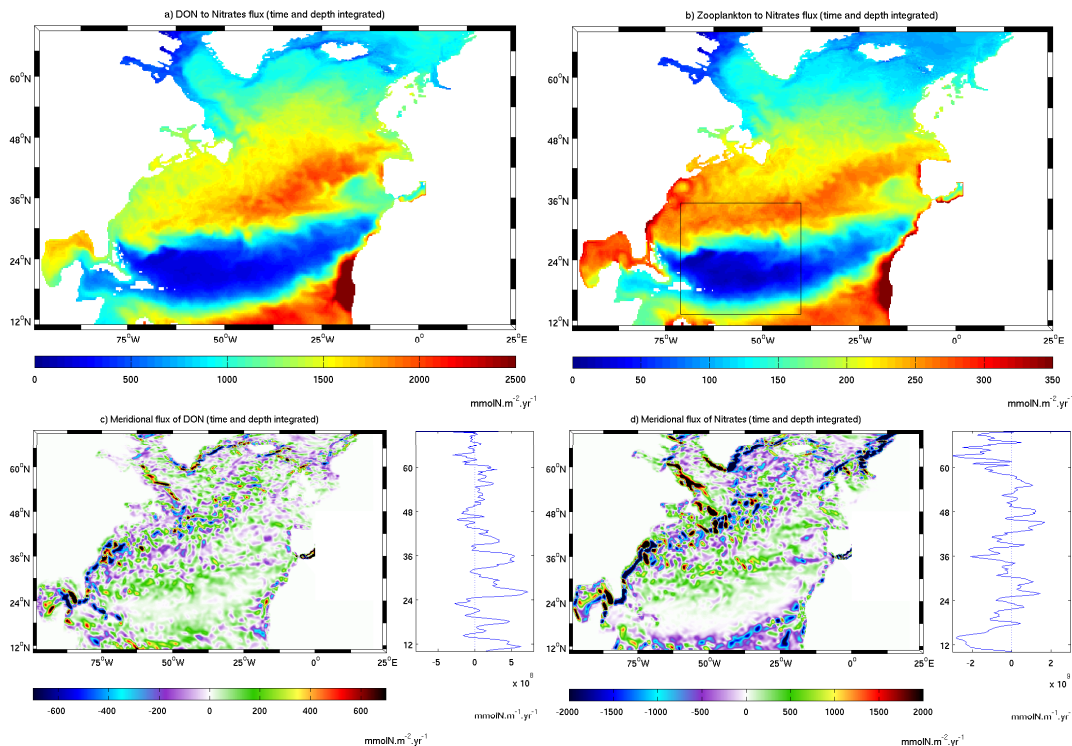


**Fig. 9.** Spatial distribution integrated over the first 112 m and over the year 1998 in  $\text{mmolN.m}^{-2}.\text{yr}^{-1}$  of (a) remineralisation of DON ( $0\text{--}2500\text{ mmolN.m}^{-2}.\text{yr}^{-1}$ ) (b) zooplankton excretion ( $0\text{--}350\text{ mmolN.m}^{-2}.\text{yr}^{-1}$ ) (c) meridional advective flux of DON ( $-700\text{--}700\text{ mmolN.m}^{-2}.\text{yr}^{-1}$ ) (d) meridional advective flux of nitrate ( $-2000\text{--}2000\text{ mmolN.m}^{-2}.\text{yr}^{-1}$ ). The black rectangle on panel (b) represents the region from 13° N to 35° N and from 71° W to 40° W where the budgets are estimated. The right panels associated to maps (c) and (d) are representing the corresponding zonally integrated fluxes over the basin.

Title Page

Abstract

Introduction

Conclusions

References

Tables

Figures

◀

▶

◀

▶

Back

Close

Full Screen / Esc

Printer-friendly Version

Interactive Discussion



## Dissolved Organic Nitrogen and primary production

G. Charria et al.

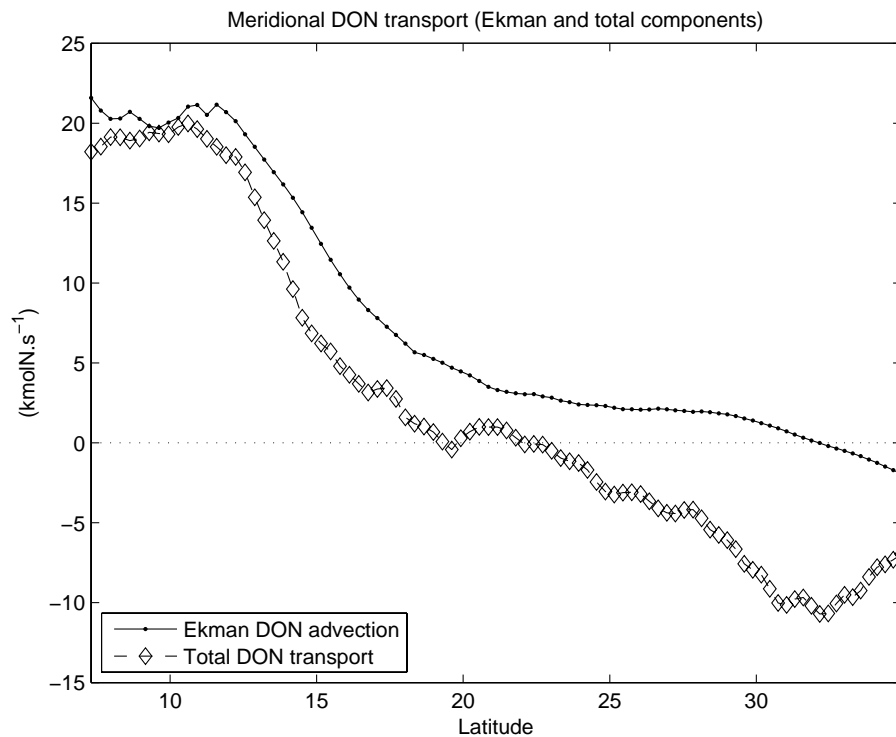


**Fig. 10.** Meridional transport of DON zonally integrated from 71°W to the eastern boundary (dashed line) and meridional Ekman transport of DON (solid line) in  $\text{kmolN}\cdot\text{s}^{-1}$ . The positive values represent a northward transport.

Title Page

Abstract

Introduction

Conclusions

References

Tables

Figures

◀

▶

◀

▶

Back

Close

Full Screen / Esc

Printer-friendly Version

Interactive Discussion



Dissolved Organic Nitrogen and primary production

G. Charria et al.

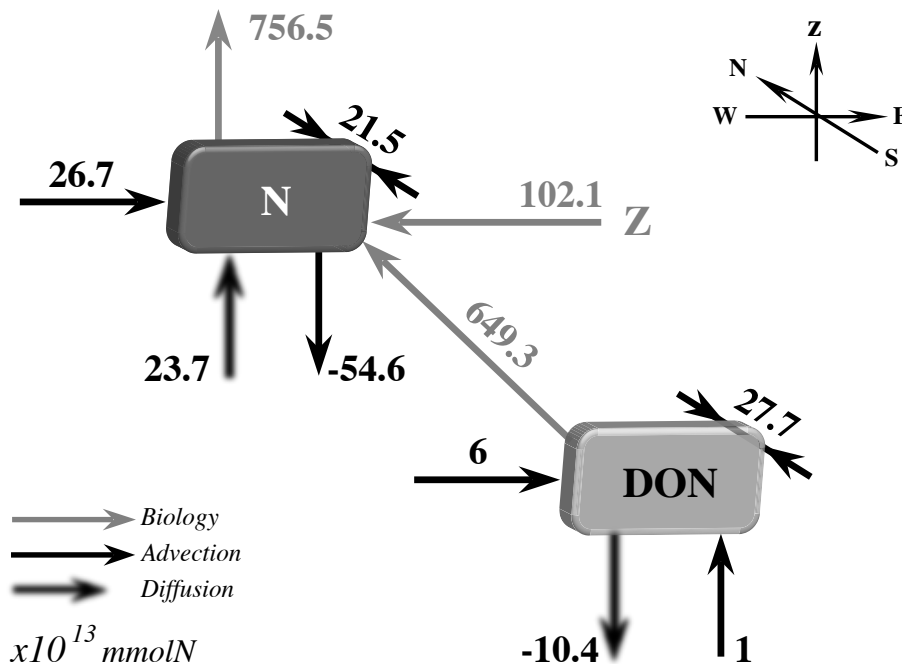


**Fig. 11.** Budget of sources and sinks (advective, diffusive and biogeochemical) of dissolved inorganic nitrogen and dissolved organic nitrogen over a given area (between 13° N and 35° N and between 71° W and 40° W) for the first 112 m during the year 1998.

Title Page

Abstract Introduction

Conclusions References

Tables Figures

◀ ▶

◀ ▶

Back Close

Full Screen / Esc

Printer-friendly Version

Interactive Discussion

